

Design and analysis of a magnetically levitated axial flux BLDC motor for a ventricular assist device (VAD)

Ahmet FENERCİOĞLU*

Department of Mechatronics Engineering, Faculty of Engineering and Natural Science, Gaziosmanpaşa University, Tokat, Turkey

Received: 22.05.2014

Accepted/Published Online: 27.12.2014

Final Version: 15.04.2016

Abstract: This study presents the design of a magnetically levitated (maglev) axial magnetic flux brushless direct current motor (AF-BLDC) for an axial blood flow ventricular assist device (VAD). It has three phases, twelve salient stator poles, and eight rotor magnet poles. It is designed in miniature size. Twin AF-BLDC motors are placed in the VAD symmetrically and rotors are coupled to the pump from two sides. The stator and rotor of the proposed motor are designed with a hole since magnetic flux does not pass through the central part. Pump impellers may be placed in this hole for larger pump chamber volume and lower speed. The motor has a passive magnetic bearing and does not involve contact and friction to minimize blood damage. Bearing magnets ensure magnetic suspension. Axial magnetic fluxes are parallel to blood flow direction, thus minimizing penetration of magnetic field into blood. Magnetic parameters, axial pull force, and torque of the proposed motor have been analyzed by the 3-dimensional finite elements method (3D-FEM) to confirm the motor design. Solutions are compared with maglev and non-maglev designs.

Key words: Axial flux BLDC motor design, maglev bearing, VAD motors

1. Introduction

According to the World Health Organization, cardiovascular diseases are a major cause of death in industrialized countries. Heart transplantation is one of the therapy options for patients suffering from terminal heart failure, and is dependent on the available number of donor hearts. It is due to this issue that many patients die while waiting for a donor organ [1]. In order to sustain the patients' life, VAD can mechanically support the human heart to achieve a sufficient perfusion of the body [2].

According to blood outflow, VAD's are generally classified in two groups: volume displacement (pulsatile) and continuous flow. Continuous flow VADs have two different pump types: radial (centrifugal) and axial flow. Recent studies focus on the bearingless maglev VAD, which is also called the 3rd generation [3]. VADs should have a very durable, light, and compact structure [4] as they are implanted into the human body through surgical methods. Tissue compatible material should be used in places of contact with blood. No damage should be given to blood for hemolysis and clotting. It should have low power and low energy consumption due to heating. A major part of these problems regarded as an important risk for VADs has been reduced with the changes provided in pump design only [5]. Generally radial magnetic flux BLDC motors are used in axial blood flow VADs. Permanent magnets are embedded in pump impellers. In radial flux BLDC motors, magnetic flux is

*Correspondence: ahmet.fenercioglu@gop.edu.tr

perpendicular to blood flow. As blood hemoglobin includes iron, there are some studies in the literature stating that the magnetic field has a negative impact on blood [6]. In the literature [2] a hybrid permanent magnet hydrodynamic bearing is designed. It works passively and is contactless. Various permanent magnet topologies are studied and analyzed by FEM in terms of axial forces and stiffness [2]. In the literature [4] an axial-type self-bearing motor is proposed with a levitated rotor for a small blood pump. The axial type motor consists of two stators with six poles, a rotor with four permanent magnets on both sides, and an axial magnetic bearing controlling both the rotation and the axial translation of the rotor. The radial and tilt directions rely on passive stability and so the rotor has poor damping, which might cause blood damage. The proposed design has a hydrodynamic bearing to improve radial support properties. An experimental prototype has been constructed and incorporated into a mixed flow blood pump to confirm its functionality. The bidirectional axial-type self-bearing motor had high efficiency as a small continuous flow blood pump, delivering sufficient flow rate and pressure head. The study [5] adopts electromagnetic and fluid FEA (finite element analysis) proposing a method for the design of the magnetic suspension and impeller of an axial flow blood pump. The characteristics of the magnetic bearing are verified by electromagnetic FEM analysis. The impellers have been designed for different ways of thickening the impeller and simulated. In conclusion the impeller thickened with certain rules has better characteristics in the same conditions. The literature [7] presents the novel design and optimization of an axial flux motor for blood pump application. Different design topologies of an axial flux permanent magnet (AFPM) machine have been examined to maximize motor efficiency. Halbach arrangement of rotor magnets and use of soft magnetic composite (SMC) material in the core provide advantages to optimal motor design. Torque, losses, and flux density results of the proposed motor are obtained by 3D FEM analysis. The literature [8] proposes a novel design with a degree of freedom of one actively positioned bearingless motor. It is based on an axial flux motor where field weakening and strengthening with d-axis current modulation produce the suspension force for axial motion control. The single drive bearingless motor does not require additional windings and inverters. It has only three phase coils and an inverter. This novel proposal is verified by theoretical calculations, FEM analysis, and prototype model experiments. The literature [9–11] presents the design and implementation of a magnetically levitated axial blood pump. The rotor has a hollow structure for blood flow and an impeller is placed on the pump rotor inner surface. The magnetic levitation is realized using two passive magnetic bearings for radial direction balancing and an electromagnetic actuator for axial direction balancing. A sensor assembly for the rotor's axial position control is also presented [10].

In the VAD, the anticipated major problem is blood damage. Because the volume of the pump chamber is smaller in the axial flow VADs, it needs a high speed rotor. For this reason it causes blood damage due to high shear stress. The proposed design has larger volume of the pump house than conventional VADs and so the pump rotor rotates at lower speeds for the same pumped blood amount per minute. Therefore, shear stress is reduced in blood. In the proposed motor, magnetic flux is not perpendicular to blood flow and so the magnetic field does not affect blood negatively.

This study presents a proposal and FEA of magnetically levitated axial flux twin BLDC motors for an axial blood flow VAD. This proposal takes inspiration from the Berlin INCOR®[3] and Yang and Huang's VAD in the literature [9–11] and it is proposed as a combination of both. It does not consist of mechanical, computational fluids dynamic (CFD) analyses, and system control due to verified models. Motors are placed symmetrically and rotors are coupled to the pump from two sides. The stator and rotor of the AF-BLDC motor have been left with a hole as magnetic flux does not pass through the central section. Pump impellers are recommended to be placed in this hole. The pump can be operated at low speed since its chamber is

bigger than those of normal axial VADs, which have impellers placed on the inner surface of the rotor. The motor is designed with a magnetic bearing and does not involve contact and friction. Passive bearing magnets are placed in the motor to ensure maglev. Motors can be independently controlled with field weakening or strengthening to assist magnetic suspension [8]. Magnetic parameters, force, and torque have been analyzed through the three-dimensional finite elements method to confirm the motor design. Solutions are compared with maglev and non-maglev designs. Axial magnetic flux direction is parallel to blood flow direction, thus minimizing penetration of blood by the magnetic field.

2. Materials and methods

Radial pumps have larger pump chambers in comparison with axial ones. There is a difference in liquid pressure between pump input and output. In contrast, axial pumps give a larger flow rate, contributing to reduced pump size. Therefore, when radial and axial pumps are used as VADs, assuming the same flow rate and liquid head for both models, the first operates with lower rotation in the rotor, but they have larger dimensions. It is equivalent to say that axial VADs make possible a more compact VAD but they demand a high speed in the rotor. Thus, both types of VADs present potential advantages and disadvantages. The reduced size is very interesting for the development of implantable VADs. However, low rotor operational speed is interesting to minimize the risk of blood damage [12].

VADs should support the human heart by providing sufficient perfusion without causing blood and tissue damage during operation. Usually the left ventricle is preferred as it has higher pressure than the right ventricle [2]. Important types of blood damage are hemolysis, thrombogenicity, clotting, and denaturation. Hemolysis is damage to blood cells by collisions with the rotor at high speed [12]. Detrimental flow structures such as areas of turbulence, stagnation, recirculation, vortices, high shear stresses, and negative pressure all contribute to increased blood damage [3]. Shear stress, stagnation, nonbiocompatible material, and coarse surfaces are the main factors that cause hemolysis and thrombocyte destruction. These effects are minimized in the design of the pump unit by basing on flow path, impeller shape, bearing, and operation speed. Hemolysis risk can be reduced with low speed and use of a no contact magnetic bearing. Denaturation starts when human body temperature reaches 40 degrees. Denaturation yields a deformation of biomolecular structure of proteins in the blood causing its destruction. Blood temperature increase may be caused by heat losses in active VAD components [2].

The literature [13] indicates that magnetic fields have negative effects on blood. Fluid parameters like blood speed, flow rate, vein wall shear stress, flow resistance, and flow acceleration are negatively affected by the magnetic field and the presence of multiple stenosis has been determined. Blood pumps implanted in the heart can be with centrifugal or axial flow.

Figure 1 presents a proposed axial flow VAD design. Literature examples have been taken into consideration as VAD design is not the subject of this study [3,9–11].

In the proposed VAD system, an impeller is symbolically placed on the inner surface of the tubular rotor. A similar design is studied for the axial flow VAD in the literature [9–11]. Symmetrically placed and passive magnetically levitated twin motor usage is proposed as a different design.

2.1. AF-BLDC motor for VAD

Permanent magnets in BLDC motors provide additional magnetic force. Therefore, they have a compact structure in comparison with the other motors that have the same power. These motors can be classified into two groups according to their magnetic flux directions as axial or radial flux. In the axial flux BLDC motor,

magnetic flux passes from stator to rotor in the rotational axis. These motors may have double or single sided stators or rotors. The proposed AF- BLDC motor has a single sided disc rotor with 8 magnets poles and stator that has three phased twelve salient poles in miniature size. Figure 2 shows the 3D simulation model.

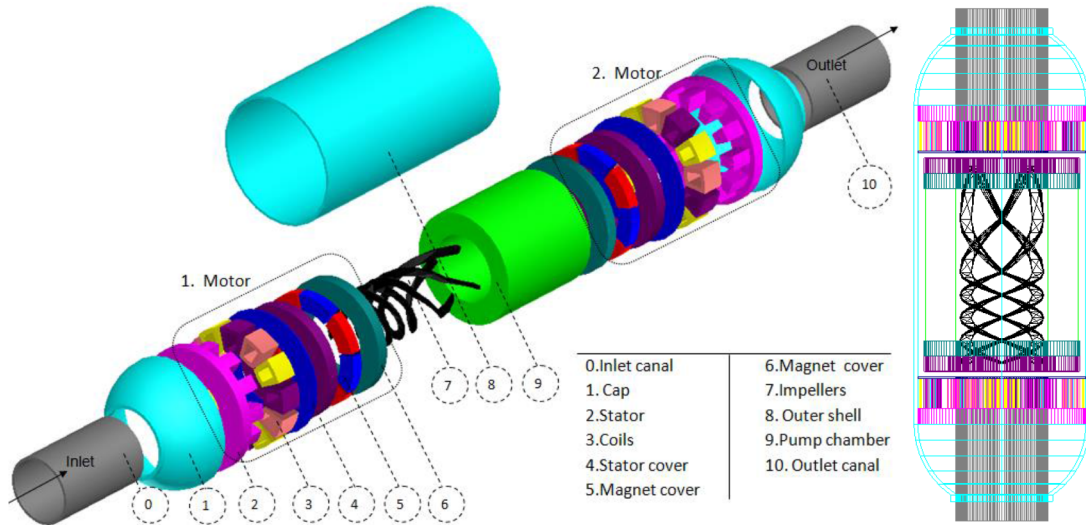


Figure 1. Proposed VAD design.

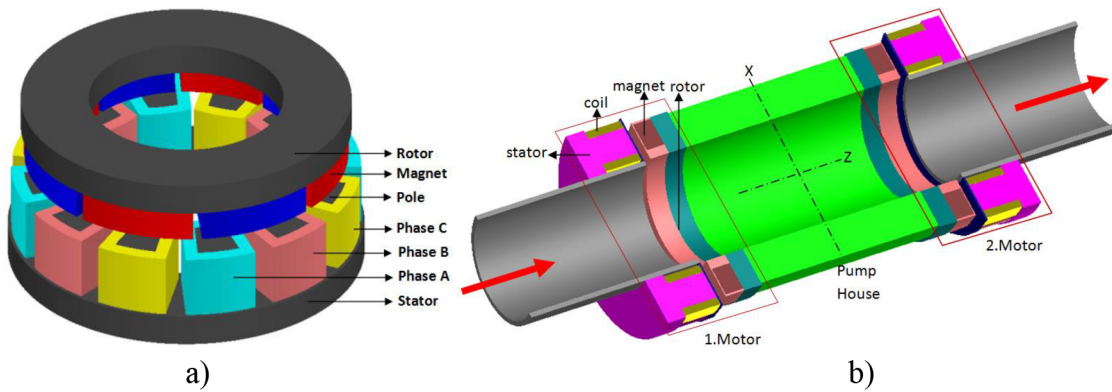


Figure 2. Simulation model a) AF-BLDC motor, b) Twin AF-BLDC motor in VAD.

Since structurally no flux passes through the center of the stator and the rotor, it can be left as a hole. Due to this advantage, it is proposed to pass the VAD blood flow through a pipe placed in the hole in the middle of the rotor and stator. Twin BLDC motors are placed symmetrically in the VAD. This design provides an advantage for the magnetic bearing design in addition to driving the pump from both sides. Rotors are symmetrically mounted in two parts of the pump unit. In this design, the pump forms a whole with the rotors. AF-BLDC motors generate high magnitude rotor pull force (F_z) and torque generating forces (F_x , F_y). However, pull force causes friction and blockage in bearingless motors. The proposed design uses twin symmetric motors and allows magnetic bearing design by rotor forces balancing each other and it has passive bearing magnets. In addition, the pump will push the rotor in reverse direction of blood flow due to fluid dynamics during pump operation. In this sense, passive bearing magnets provide opposite push force against

the pump rotor to balance; by this way the motor is levitated magnetically. In radial flux BLDC motors, magnetic flux is perpendicular to blood flow direction. In AF-BLDC motors magnetic flux and blood flow are in the same direction. Magnetic flux completes its circuit directly in the core and does not penetrate the blood. This will reduce the harmful effects of the magnetic field on the blood. Figure 3 shows the geometrical parameters of AF-BLDC motors and Table 1 includes the size and explanations.

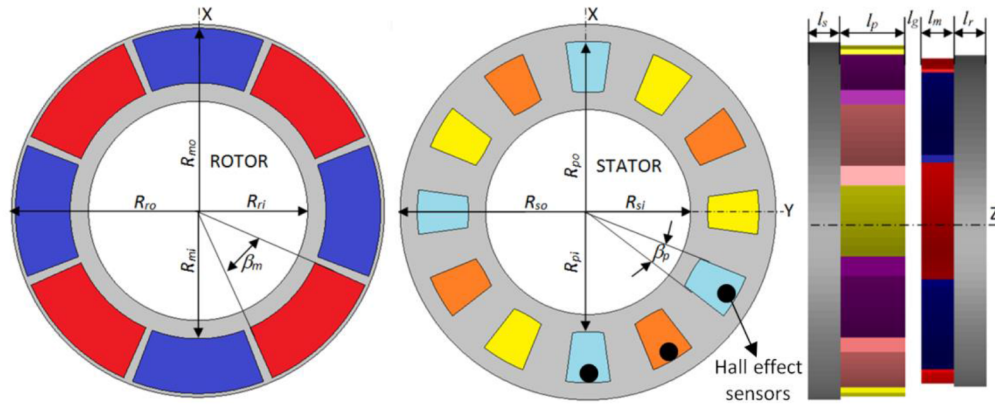


Figure 3. a) Geometrical parameters of AF-BLDC motor.

Table 1. Geometrical size and explanations of AF-BLDC motor.

Symbol	Explanations	Size (mm)
R_{so}	Outer radius of stator	11
R_{si}	Inner radius of stator	6
R_{po}	Outer radius of stator poles	10
R_{pi}	Inner radius of stator poles	7
R_{ro}	Outer radius of rotor	10.2
R_{ri}	Inner radius of rotor	6
R_{mo}	Outer radius of magnets	10
R_{mi}	Inner radius of magnets	7
l_s	Stator yoke thickness	2
l_p	Stator pole length	4
l_g	Airgap distance	1
l_m	Magnet height	2
l_r	Rotor yoke thickness	2
β_m	Angle of magnet	42°
β_p	Angle of poles	30°
m	Phase number	3
n_p	Pole number	8
a_m	Magnet embrace	0.93

The proposed motor has three phases and star connections. During operation, two phases are simultaneously excited according to rotor position and direction. There is no excitation in another remaining phase. Excited phase current directions are opposite to each other. Magnetic flux path of the motor in the state of excitation of Phase A and B is given in Figure 4.

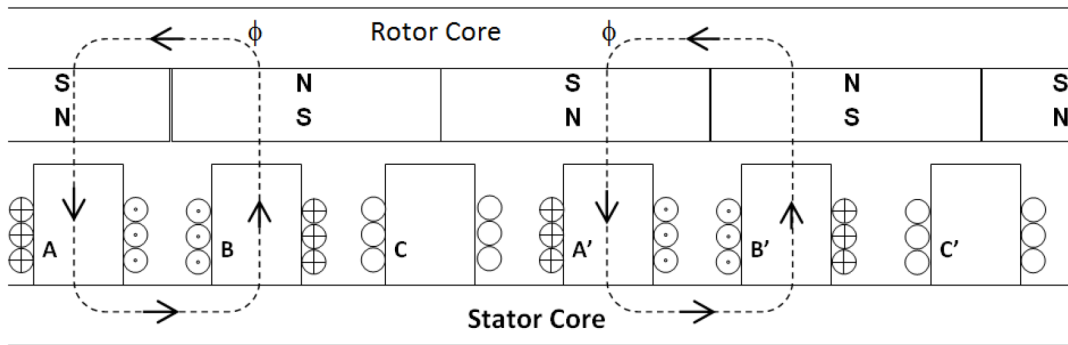


Figure 4. Flux path of AF-BLDC motor.

Sequence of phase to be switched depends on the direction and rotor position. Rotation is in a single direction as the motor is proposed for driving a blood pump. Due to the 12-pole stator, rotor position information is taken from Hall effect sensors that are embedded in the stator at an angle of 30° . The rotor rotates by 30° for each phase excitation. As the magnetic permeability of the core is considered to be infinite, core reluctance is zero. Air gap reluctance R_g and permanent magnet reluctance R_m are calculated with Eq. (1) [8].

$$R_g = \frac{l_g}{\mu_0 S}, R_m = \frac{l_m}{\mu_m S}, \tag{1}$$

where l_g is air gap distance and l_m is magnet length. S is the effective surface area of the stator pole. When the permeability of magnet is taken equal to the permeability of the magnet ($\mu_m = \mu_0$) total reluctance R_0 is calculated with Eq. (2) [8].

$$R_0 = R_g + R_m = \frac{l_g + l_m}{\mu_0 S} \tag{2}$$

In this case we obtain permeance ρ_0 expression from Eq. (3) [8].

$$\rho_0 = \frac{1}{R_0} = \frac{\mu_0 S}{l_g + l_m} \tag{3}$$

Magnetomotive force (mmf) of the magnetic circuit according to the air gap and field magnitudes of magnets is calculated using Eq. (4) in accordance with Ampere's law.

$$Ni = (H_m l_m + H_g l_g) \tag{4}$$

Magnetic flux density \emptyset is obtained with Eq. (5) [14].

$$\emptyset = B_m A_m = B_g A_g = \mu_0 H_g A_g \tag{5}$$

Magnetic flux density is derived from Eq. (5) and is calculated by Eq. (6) [14].

$$B_m = -\mu_0 \left(\frac{A_g}{A_m} \right) \left(\frac{l_m}{l_g} \right) H_m + \frac{\mu_0 N}{l_g} \left(\frac{A_g}{A_m} \right) I \tag{6}$$

Current to be applied according to B_m and H_m values by taking the operation range of the magnet into consideration is calculated with Eq. (7) [14].

$$I = \left(B_m + \mu_0 \left(\frac{A_g l_m}{A_m l_g} \right) H_m \right) \left(\frac{A_m l_g}{\mu_0 N A_g} \right) \tag{7}$$

Basically torque can be calculated using Eq. (8) through the multiplication of rotor diameter R_{ro} with radial force F_{rad} [2,15].

$$\vec{T} = \vec{R}_{ro} \times \vec{F}_{rad} \quad (8)$$

Radial force F_{rad} , which generates torque, is obtained through Eq. (9) and axial force, which is applying pull force to rotor F_{ax} , is obtained by Eq. (10) [2,15].

$$\vec{F}_{rad} = I \left(\vec{l} \times \vec{B}_g \right) \vec{e}_{rad} \quad (9)$$

$$\vec{F}_{ax} = \frac{B_g^2 \cdot A}{2\mu_0} \vec{e}_{ax} \quad (10)$$

In motor geometry, active coil length is l and I is the current applied to coil. B_g is the air gap magnetic flux density [2]. Axial force is the pull force of the rotor. In magnetic bearing motors, this force causes friction and blockage if it is not compensated. The proposed system design uses symmetrically placed twin motors and passive bearing magnets; therefore basic axial forces generated by motors compensate each other in unloaded operation. Due to the dynamics of the pumped liquid in loaded operation, the pump rotor will be pushed in reverse direction depending on the motor speed and liquid viscosity. This force can be compensated by bearing magnets. In this case axial balance is ensured by bearing magnets in a maglev design, which is presented in Figure 5.

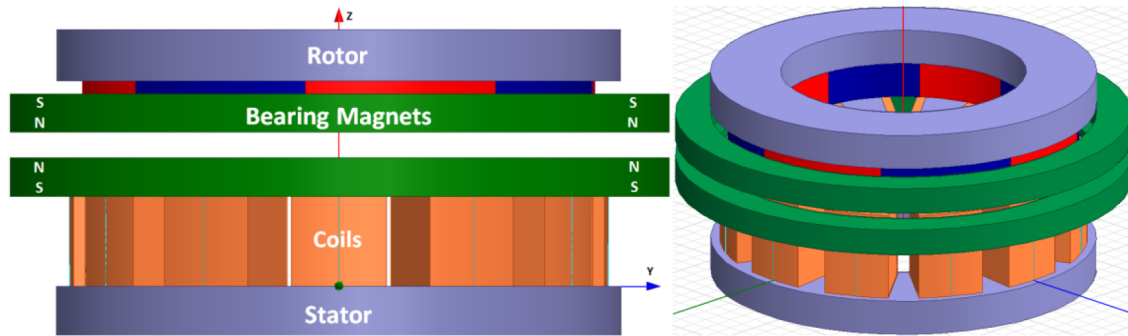


Figure 5. Maglev design of AF-BLDC motor.

2.2. Finite element analysis (FEA)

3D magnetostatic analyses of proposed motor were carried out with ANSYS Maxwell FEA software. Magnetomotive forces (mmf) were applied at A and B phases of the motor. There are four windings for each phase as there are twelve poles and windings. 80, 100, and 120 Amper-turn (At) mmf were applied two phases in different directions. Turn of a coil is accepted as 40 turns. In this case phase currents are respectively 2, 2.5, and 3 A. 80 At mmf is the unsaturated region of the core and near to linear. 100 At excitation is the knee point of the BH curve and the beginning of saturation. 120 At excitation is located in the saturated region. These mmf values were determined by taking BH curve of the core material into consideration. Figure 6 shows the BH curve of the material (Steel 1008) in the simulation model.

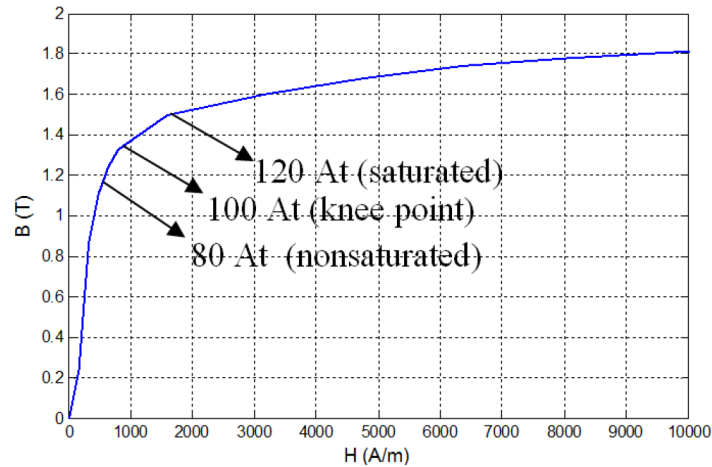


Figure 6. BH curve of core material.

Passive bearing and rotor pole magnets are selected as NdFe35 from Maxwell library. Magnets fields are defined in the axial direction and its specifications are given in Table 2.

Table 2. NdFe35 magnet specifications.

Relative permeability	1.0998
Bulk conductivity	625,000 S/m
Magnetic coercivity	Vector
H magnitude	890.000 A/m
Maximum working temp	100 ° C

As the motor rotated 30° in one phase excitation period, the rotor was rotated by angles of 3° in 11 steps. The instantaneous value of force and torque were calculated for each rotor position by magnetostatic FEA. As each excitation period is the same, solutions for one period are sufficient. Axial forces (F_x , F_y) other than the shaft axis generate torque. Force in the shaft axis (F_z) is the rotor pull force of the stator and is shown in Figure 7. The pull forces have the same magnitude but different directions in the symmetrically placed twin motors and so that these forces balance each other. This provides an advantage for magnetic bearing. F_{mg} is magnet repel force to ensure maglev.

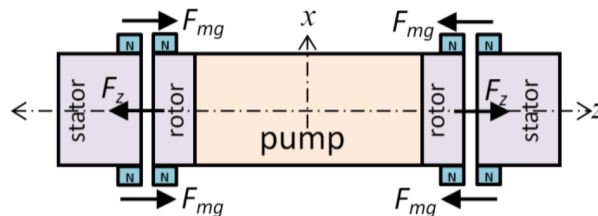


Figure 7. Shaft axis pull force (F_z)

3. Results and discussions

F_z forces according to 0, 2, 2.5 and 3 Ampere phase currents in each 3° rotor position are calculated with magnetostatic FEA for maglev and non-maglev designs. In non-maglev state without excitation average pull force (F_z) is -11.1385 N; in maglev state it is 0.4311 N. Thus bearingless operation is possible as pull force is

compensated by bearing magnets and average F_z is positive in the maglev design. It is negative and higher magnitude in the non-maglev design for all excitations. It is compared in Table 3 and shown by graphics for the 2.5 A phase excitation in Figure 8.

Table 3. Average pull force (N) comparisons.

Phase current	F_z , average pull force (N) (0–30° rotor positions)	
	Maglev	Non-maglev
0 A	0.4311	-11.1385
2 A	0.5267	-11.0817
2.5 A	0.5423	-11.0840
3 A	0.5565	-11.0876

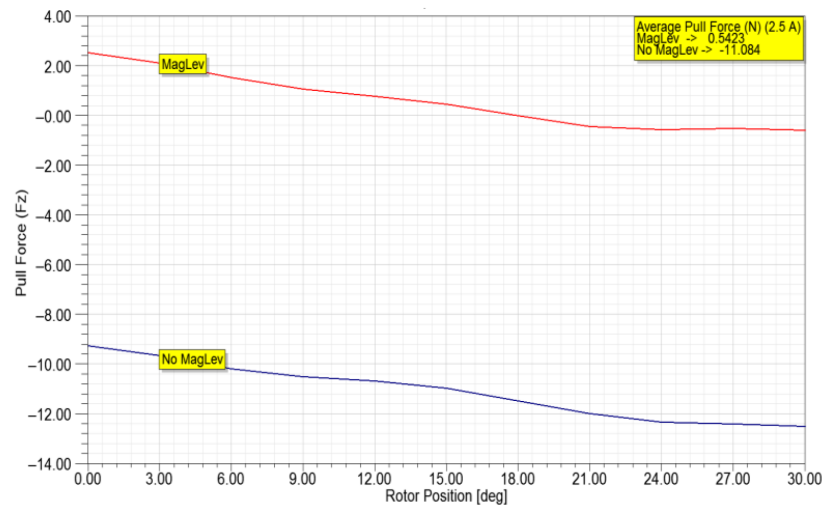


Figure 8. F_z forces for one AF-BLDC motor under the 2.5 A phase excitation.

In rotor positions between 0° and 15° , it is observed that pull force decreases as current increases as magnet fields and core fields are in opposite directions. In rotor positions between 15° and 30° F_z force is increased as current increases. Magnet fields and core flux are in the same directions; thus magnets strengthen total magnetic field. Another symmetrically placed another twin motor generates the same forces in reverse direction and therefore the system will operate with magnetic bearing by providing a balance in the unloaded operation. However, it is unbalanced in loaded pump operations due to fluid dynamics. The rotor is pushed in reverse of the fluid flow direction. This will cause friction and blockage. It depends on pump speed. In this case, balance is ensured by passive bearing magnets and separately controlling the twin motors. If maglev magnets forces may not be compensated against the fluid push forces in a very high speed bearing, the volume of the magnet placed in the opposite flow direction should be enlarged. In addition, magnetic bearing supports with circular magnets provide balance in an axis other than the shaft axis. Electromagnetic torque results were calculated under 2, 2.5, and 3 Ampere phase excitation. A rippled torque is observed since these are instantaneous magnetostatic torque values. Less rippled torque results are obtained due to the inertia of the rotor in dynamic operation at high speeds. Electromagnetic shaft torque is presented in Figure 9 for maglev and non-maglev designs under the 2.5 A excitation. The average torque is compared in Table 4 for all excitations. The average electromagnetic torque is reduced less than 2% in the maglev design as the total core magnetic field is affected by bearing magnets.

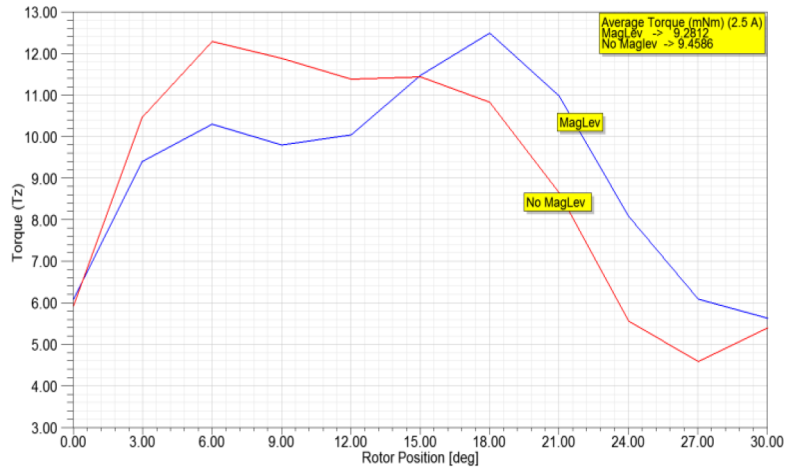


Figure 9. Single AF-BLDC motor torque profile.

Table 4. Electromagnetic torque and power comparisons in maglev and non-maglev.

Phase current	T_z , average torque (mNm) Rotor positions : 0–30°		Power (W) Speed: 4500 rpm	
	Maglev	Non-maglev	Maglev	Non-maglev
0 A	0	0	0	0
2 A	7.5288	7.7224	3.55	3.64
2.5 A	9.2812	9.4586	4.37	4.46
3 A	11.0507	11.2222	5.20	5.29

The axial flow VADs operate at high speeds. The literature includes VADs operating at speeds between 3000 and 12,000 rpm. They can pump 5 L of blood per minute at speeds of 5000–6000 rpm. In general, a high speed is required for axial flow VADs due to the volume of the small pump house. Torque in pump loads of especially electric motors is proportional with the square of speed; power is proportional with the cube of speed. Magnetic flux density distribution in the motor is solved with FEA for 2.5 A DC excitation and 0° rotor position. Results are given in Figure 10 with respect to magnitude and vector.

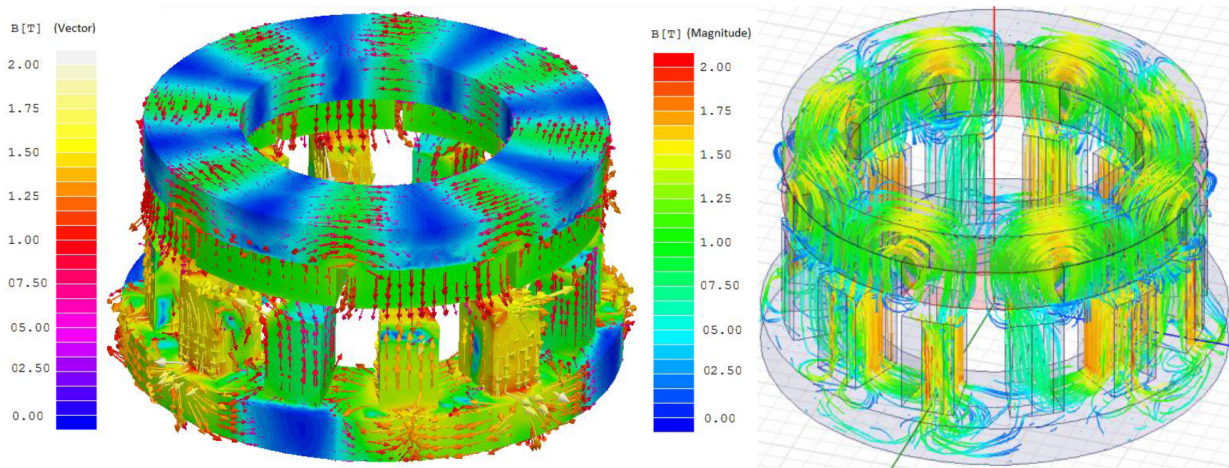


Figure 10. Magnetic flux density distribution.

Flux density in excited stator poles is around 1.5 T. Local saturation is observed in pole edges. There is a nonuniform flux distribution on the stator and rotor. Therefore, flux is weakened in some parts. When vectorial flux directions are considered, magnetic circuits are observed. Magnetic flux in the VAD's radial motors is perpendicular to blood flow and they may have negative effects on blood [6]. The literature reviews negative effects of magnetic flux on blood and they are within acceptable limits. Magnetic flux in AF-BLDC motors is axial and in the same direction with blood flow. Thus it will not damage blood as magnetic flux does not directly penetrate the blood.

4. Conclusion

An AF-BLDC motor design was proposed for axial blood flow VADs with magnetic bearing. This motor has miniature size and includes a hole in the central part. Inlet, outlet channels, and impellers were placed in this hole for blood flow. As the compact design is one of the most significant aspects of the VAD, it may be proposed for pediatric patients. A three-phased AF-BLDC motor has 12 salient stator poles and the rotor has 8 NdFeB magnet poles. Rotors were symmetrically placed in the pump chamber. Twin motors balanced axial pull forces mutually. The motor was analyzed with ANSYS Maxwell 3D FEA software to calculate magnetic parameters, torque, force, and power. Analyses were done for 0–30 degree rotor positions with one phase excitation period. Axial pull force and torque were calculated for maglev and non-maglev designs. Accordingly, average torque was calculated 11.05 mNm under the 3 A phase excitation, and power for 4500 rpm speed including all losses was 5.20 W for the single magnetically levitated AF-BLDC motor. The stator average pull force (F_z) was solved: 11.1385 N in non-maglev state and 0.4311 N in maglev state without excitation. Thus bearingless operation is possible as pull force is compensated by bearing magnets. Furthermore, axial pull force was balanced by mutually placed twin motors. In addition magnetic field weakening or strengthening can be assisted in maglev with separately controlled twin motors. The average electromagnetic torque is reduced less than 2% in the maglev design as total core magnetic field is affected by bearing magnets. A passive maglev bearing does not require a complex control algorithm and sensing tilt. The most important parameter for VADs is shear stress, which causes blood damage. This harmful effect is minimized with a bearingless pump design.

References

- [1] Pohlmann A, Lesmann, M, Hameyer K. Comparative study on optimization methods for a motor-drive of artificial hearts. *International Conference on Electrical Machines and Systems (ICEMS)*; 10–13 October 2010; Incheon: pp. 1754-1758.
- [2] Pohlmann A, Hameyer K. A study on permanent magnet topologies for hybrid bearings for medical drives applied in Ventricular Assist Devices. *Archives of Electrical Engineering* 2011; 60: 371-380.
- [3] Timms D. A review of clinical ventricular assist devices. *Medical Engineering & Physics* 2011; 33: 1041-1047.
- [4] Okada Y, Yamashiro N, Ohmori K, Masuzawa T, Yamane T, Konishi Y, Ueno S. Mixed flow artificial heart pump with axial self-bearing motor. *IEEE/ASME Transactions on Mechatronics* 2005; 10: 658-665.
- [5] Wu H, Wang Z, Lv X. Design and simulation of axial flow maglev blood pump. *Int. Journal of Information Engineering and Electronic Business* 2011; 2: 42-48.
- [6] McKay J C, Prato F S, Thomas A W. A literature review: the effects of magnetic field exposure on blood flow and blood vessels in the microvasculature. *Bioelectromagnetics* 2007; 28: 81-98.
- [7] Neethu S, Shinoy KS, Shajilal AS. Novel design, optimization and realization of axial flux motor for implantable blood pump. *Power Electronics, Drives and Energy Systems (PEDES) & 2010 Power India*. 2–23 December 2010; New Delhi, India. pp. 1-6.

- [8] Asama J, Hamasaki Y, Oiwa T, Chiba A. Proposal and analysis of a novel single-drive bearingless motor. *IEEE Transaction on Industrial Electronics* 2013; 60: 129-138.
- [9] Yang SM, Huang CL. Design of a new electromagnetic actuator which can produce three-dimensional forces. *IEEE Transaction on Magnetics* 2009; 45: 4153-4156.
- [10] Yang SM. Design and implementation of a magnetically levitated single-axis controlled axial blood pump. *IEEE Transactions on Industrial Electronics* 2011; 58: 611-617.
- [11] Yang SM. Electromagnetic actuator implementation and control for resonance vibration reduction in miniature magnetically levitated rotating machines. *IEEE Transactions on Industrial Electronics* 2011; 58: 611-617.
- [12] Horikawa O, Andrade AJP, Silva I, Bock EGP. Magnetic suspension of the rotor of a ventricular assist device of mixed flow type. *Artificial Organs* 2008; 32: 334-341.
- [13] Varshney G, Katiyar VK, Kumar S. Effect of magnetic field on the blood flow in artery having multiple stenosis: a numerical study. *International Journal of Engineering, Science and Technology* 2010; 2: 67-82.
- [14] Fitzgerald AE, Kingsley C, Umans SD. *Electric Machinery*. 6th ed. New York, NY, USA: McGraw-Hill, 2002.
- [15] Polhman A, Lesmann M, Hamayer K. Algorithm-based drive design for a ventricular assist device. *The International Journal for Computation and Mathematics in Electrical and Electronic Engineering* 2012; 31: 1067-1076.